Charge order and spin-singlet pair formation in Ti_4O_7

2006 J. Phys.: Condens. Matter 18 10955

(http://iopscience.iop.org/0953-8984/18/48/022)

INSTITUTE OF PHYSICS PUBLISHING JOURNAL OF PHYSICS: CONDENSED MATTER

J. Phys.: Condens. Matter **18** (2006) 10955–10964 doi:10.1088/0953-8984/18/48/022

Charge order and spin-singlet pair formation in Ti_4O_7

I Leonov[1], A N Yaresko[2], V N Antonov[3], U Schwingenschlögl[4], V Eyert[4] and V I Anisimov[5]

[1] Theoretical Physics III, Center for Electronic Correlations and Magnetism, Institute for Physics, University of Augsburg, Germany
[2] Max-Planck Institute for the Physics of Complex Systems, Dresden, Germany
[3] Institute of Metal Physics, Vernadskii Street, 03142 Kiev, Ukraine
[4] Theoretical Physics II, Institute for Physics, University of Augsburg, Germany
[5] Institute of Metal Physics, Russian Academy of Science—Ural Division, 620219 Yekaterinburg GSP-170, Russia

E-mail: Ivan.Leonov@Physik.uni-Augsburg.de

Received 23 August 2006
Published 17 November 2006
Online at stacks.iop.org/JPhysCM/18/10955

Abstract

Charge ordering in the low-temperature triclinic structure of titanium oxide (Ti_4O_7) is investigated using the local density approximation (LDA) + U method. Although the total 3d charge separation is rather small, an orbital order parameter defined as the difference between t_{2g} occupancies of Ti^{3+} and Ti^{4+} cations is large and gives direct evidence for charge ordering. Strong covalency of O 2p–Ti 3d σ-type bonds, which results in partial occupation of Ti e_g states, leads to almost complete loss of the disproportionation between the charges at 3+ and 4+ Ti sites. The occupied t_{2g} states of Ti^{3+} cations are predominantly of d_{xy} character and form a spin-singlet molecular orbital via strong direct antiferromagnetic exchange coupling between neighbouring Ti(1) and Ti(3) sites, whereas the role of superexchange is found to be negligible.

(Some figures in this article are in colour only in the electronic version)

1. Introduction

The mixed valent transition metal oxides, which simultaneously contain metal atoms in two (or more) different valence states, are of strong current interest [1]. One of the classical examples of such a system is magnetite (Fe_3O_4), in which a first-order metal–insulator transition occurs at ∼120 K [2]. According to Verwey, this transition is caused by the spatial ordering of 2+ and 3+ Fe cations on the octahedral B-sublattice of the inverted spinel structure AB_2O_4 [3, 4]. Recently, a local spin density approximation (LSDA) + U study of the low-temperature phase of Fe_3O_4 resulted in a charge and orbitally ordered insulating ground state with a well-pronounced orbital order [5, 6]. However, the strong difference in t_{2g} occupancies of 2+ and

3+ Fe was found to be drastically reduced by effective 'static' screening[6]. A similar result (see [7]) has been obtained for another iron oxide, containing both 2+ and 3+ Fe cations, iron oxoborate (Fe_2OBO_3), which shows a broad semiconductor-to-semiconductor transition at ∼317 K associated (as in Fe_3O_4) with a spatial order–disorder transformation of 2+ and 3+ Fe cations on quasi-one-dimensional Fe chains [8–10].

The aforementioned phenomena of sharp metal–insulator transitions associated with pronounced charge and/or orbital ordering are characteristic for the *Magnéli* phases M_nO_{2n-1} (M = Ti, V).[7] These compounds form a homologous series and have been studied recently to understand the differences in crystal structures and electronic properties between the end members MO_2 ($n \to \infty$) and M_2O_3 ($n = 2$) [11]. In particular, the metal–insulator transition of VO_2 discovered some 50 years ago is still the subject of ongoing controversy and is another 'hot topic' in solid-state physics. LDA calculations have revealed a strong influence of the structural degrees of freedom on the electronic properties of VO_2 and neighbouring rutile-type dioxides [12–16]. In this scenario the characteristic dimerization and antiferroelectric displacement of the metal atoms translate into orbital ordering within the t_{2g} states and a Peierls-like singlet formation between neighbouring sites. Recently, this was confirmed by LDA + DMFT calculations, which suggested regarding the transition of VO_2 as a correlation-assisted Peierls transition [17].

Ti_4O_7 titanium oxide is another remarkable member of the *Magnéli* phases with $n = 4$ which shows metal–insulator transitions associated with the spatial charge ordering. It is a mixed valent compound which has an even mixture of 3+ and 4+ Ti cations ($Ti_2^{3+}Ti_2^{4+}O_7$), corresponding to an average 3d occupation of $1/2$ electron per Ti site. Electrical resistivity, specific heat, magnetic susceptibility, and x-ray diffraction data reveal two first-order transitions in the temperature range of 130–150 K [18–20]. At 150 K a metal–semiconductor transition occurs without measurable hysteresis in the resistivity and specific heat. It is followed by a semiconductor–semiconductor transition at 130–140 K, which again is characterized by an almost two orders of magnitude abrupt increase in electrical resistivity and has a hysteresis of several degrees [18, 19]. The magnetic susceptibility shows a sharp enhancement when heating through 150 K. However, it is small and temperature independent below this temperature and does not show any anomaly at 140 K.

The crystal structure of Ti_4O_7 (see figure 1) can be viewed as rutile-type slabs of infinite extension and a thickness of four Ti sites, separated by shear planes with a corundum-like atomic arrangement. Below 130 K it crystallizes into a triclinic crystal structure with two formula units per primitive unit cell [21–23]. Four crystallographically inequivalent Ti sites are found at the centres of distorted oxygen octahedra. They form two types of chains, namely (*a*) 1–3–3–1 and (*b*) 2–4–4–2, which run parallel to the pseudo-rutile *c*-axis and are separated by the crystallographic shear planes. Although interatomic distances in the *b* chain are almost uniform (3.01 and 3.07 Å between 4–4 and 2–4 Ti sites, respectively), they are remarkably different for the *a* chain (3.11 and 2.79 Å between 3–3 and 1–3 Ti sites).

Accurate determination of the crystal structure allowed us to elucidate the nature of the three phases distinguished by the two first-order transitions [20–23]. In particular, in the metallic phase the average Ti–O bond lengths for crystallographically inequivalent TiO_6 octahedra are very similar, which results in the average valence state of 3.5+ per each Ti cation. Below 130 K, charge has been transferred from the *b* to the *a* chains. In addition, Ti^{3+} cations in alternate *a* chains are paired to form nonmagnetic metal–metal bonds, whereas in the intermediate phase the pairing also persists but its long-range order calls for a fivefold

[6] Here and in the following we assume a redistribution of charge between Ti t_{2g} and other states using term screening.
[7] To our knowledge of all the V_nO_{2n-1} compounds only V_7O_{13} does not exhibit a metal–insulator transition.

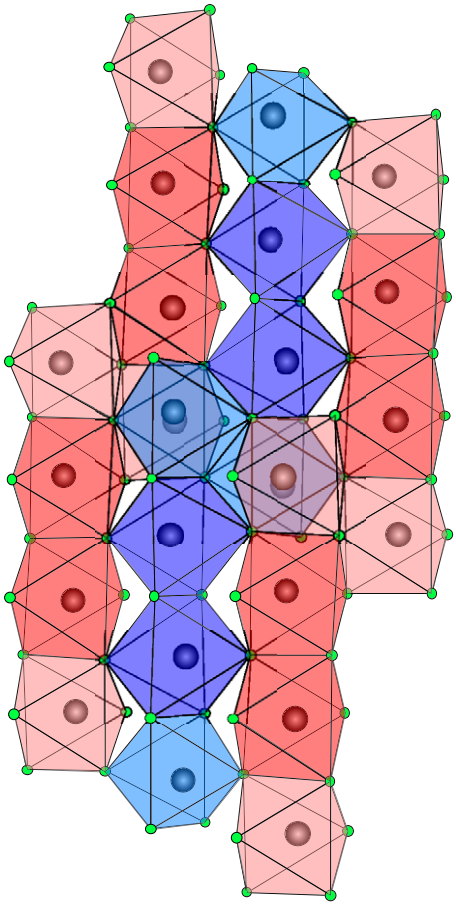

Figure 1. The low-temperature crystal structure of Ti_4O_7. Chains of four Ti sites run parallel to the pseudo-rutile *c*-axis. Red and blue (light and dark on the black and white image) chains of four Ti atoms correspond to the *a* and *b* chains of Ti atoms, respectively. Further gradation of red and blue on light and dark subsets indicates inequivalent Ti sites in *a* and *b* chains.

supercell [19]. Thus, the 130–140 K transition is associated with a transition to the phase with a long-range order of Ti^{3+}–Ti^{3+} pairs, whereas above 150 K 3+ and 4+ Ti cations are disordered. The presence of the Ti^{3+}–Ti^{3+} pairs strongly differentiates Ti_4O_7 from Fe_3O_4 and results in two steep first-order transitions found in the electrical resistivity.

Recent LDA band structure calculations of both high- and low-temperature phases of Ti_4O_7 resulted in significant t_{2g} charge separation between crystallographically independent 3+ and 4+ Ti sites in the low-temperature phase, whereas a rather isotropic occupation of the t_{2g} states has been found at room temperature [24]. While, in addition, an orbital order at the Ti d^1 chains originating from metal–metal dimerization was found, the LDA gave only a metallic solution with semimetallic-like band overlap instead of the semiconducting gap. This problem is overcome in our work, taking into account strong electronic correlations in Ti 3d shell using the LDA + U method.

In the present paper we investigate the electronic structure of the low-temperature Ti_4O_7 using the LDA + U approach [26]. The LDA + U calculations result in a charge and orbitally ordered insulator with an energy gap of 0.29 eV, which is in good agreement with

an experimental gap value of 0.25 eV. From our results, we propose an orbital order parameter, defined as the difference between t_{2g} majority/minority spin occupancies of $Ti(1)^{3+}/Ti(3)^{3+}$ and $Ti(2)^{4+}/Ti(4)^{4+}$ cations, respectively. This order parameter is found to be quite large, although the total 3d charge difference between 3+ and 4+ cations remains small. Also, it is interesting to note that the total charge separation between 3+ and 4+ Ti cations is completely lost due to efficient screening by the rearrangement of the other Ti electrons. In addition, we find a strong antiferromagnetic coupling of the local moments within the dimerized Ti^{3+}–Ti^{3+} pairs of about −1700 K, whereas an inter-pair coupling (along the a chain) is only of −81 K. This is in good agreement with small and temperature-independent magnetic susceptibility in the low-temperature phase of Ti_4O_7.

2. Computational details

The present band-structure calculations have been performed for the low-temperature triclinic structure of Ti_4O_7 [23] using the LDA + U approach [26] in the tight-binding linear muffin-tin orbital (TB-LMTO) calculation scheme [25]. The $P\bar{1}$ unit cell used in the calculations was constructed from the translation vectors of the original $I\bar{1}$ cell with $a = 5.626$ Å, $b = 7.202$ Å, $c = 20.2608$ Å, $\alpha = 67.90°$, $\beta = 57.69°$, and $\gamma = 109.68°$ found at 115 K. The radii of muffin-tin spheres were taken as $R_{Ti1-4} = 2.27$ au, $R_{O1,O3,O4-6} = 1.78$ au, and $R_{O2,O7} = 1.66$ au. Fifteen kinds of empty spheres were introduced to fill up the inter-atomic space. For simplicity, we neglect small spin–orbit coupling and consider only a collinear spin case.

3. LSDA band structure

Our LSDA band structure calculations for the low-temperature $P\bar{1}$ structure confirmed the results of the previous work [24]. The LSDA gives a nonmagnetic metallic solution with substantial charge separation between crystallographically independent Ti(1)/Ti(3) and Ti(2)/Ti(4) cations. The lower part of the valence band below −3 eV is predominantly formed by O 2p states with a bonding hybridization with Ti 3d states. Crystal field splitting of the latter is roughly of 2.5 eV. Ti t_{2g} states form the group of bands at and up to 2 eV above the Fermi energy, whereas Ti e_g states give a predominant contribution to the bands between 2.5 and 4.5 eV. Within the t_{2g} group of bands the symmetry inequivalence of Ti(1)/Ti(3) and Ti(2)/Ti(4) sites leads to substantial t_{2g} charge separation between these two groups of Ti atoms. In addition, an analysis of the partial density of states reveals significant bonding–antibonding splitting of d_{xy} (in the local cubic frame) states of about 1.5 eV for Ti(1)/Ti(3) cations, whereas Ti(2)/Ti(4) cations show a relatively weak substructure. This substantial bonding–antibonding splitting of Ti(1)/Ti(3) t_{2g} states agrees well with the concept of formation of Ti^{3+}–Ti^{3+} spin-singlet pairs proposed earlier by Marezio [19, 27]. However, the LSDA calculations fail to reproduce an insulating spin-singlet ground state of the low-temperature phase of Ti_4O_7. Apparently, the electron–electron correlations, mainly in Ti 3d shell, play a significant role.

4. LDA + U results and charge ordering

In order to take into account strong electronic correlations in the Ti 3d shell, we perform LDA+U calculations for Ti_4O_7 in the low-temperature $P\bar{1}$ structure. In our calculations we use the Coulomb interaction parameter $U = 3.0$ eV and exchange coupling $J = 0.8$ eV taken in agreement with previous constrained LDA calculations for a set of Ti-based materials [28]. The

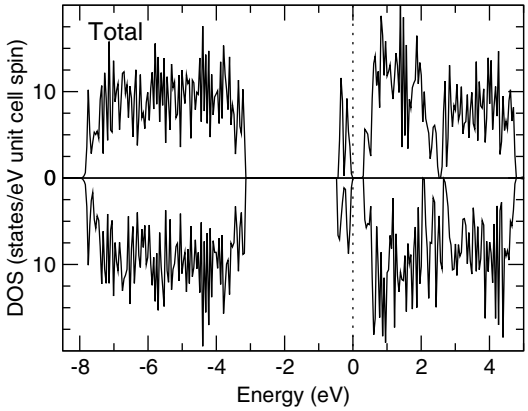

Figure 2. The total DOS obtained from LDA + U calculations with $U = 3.0$ eV and $J = 0.8$ eV for the low-temperature $P\bar{1}$ phase of Ti_4O_7. The top of the valence band is shown by dotted lines. Top and bottom panels correspond to the majority and minority spin states, respectively.

LDA + U calculations result in a charge and orbitally ordered antiferromagnetic insulator[8] with an energy gap of 0.29 eV (see figure 2). This is in strong contrast to the metallic solution with a substantial charge disproportionation between crystallographically inequivalent Ti(1)/Ti(3) and Ti(2)/Ti(4) cations obtained by LSDA and in reasonably good agreement with an experimental gap value of 0.25 eV [29]. Note, however, that the charge and orbital order pattern remains exactly the same for U in the range 2.5–4.5 eV, whereas the energy gap increases considerably up to 1.12 eV for $U = 4.5$ eV. This remarkable increase in the gap value is accompanied by the enhancement of the spin magnetic moment from 0.56 up to 0.8 μ_B per 3+ Ti(1)/Ti(3) cation as U is increased from 2.5 to 4.5 eV.

In addition, we perform LDA + U calculations for the high-temperature metallic phase of Ti_4O_7. In particular, for U in the range 2.5–3 eV the ferromagnetic metallic self-consistent solution with average occupation of 3.5+ for all Ti cations has been found. Although the calculations do not take into account possible short-range order of 3+ and 4+ Ti cations, this approximation seems to be justified by the small characteristic timescale usually observed in a charge-disordered state (see, for instance, [30] where this timescale is found to be less than 10^{-16} s in the charge-disordered phase of Fe_3O_4). With a further increase in the value of U, the metallic solution collapses into an insulating one.

After self-consistency was achieved, four crystallographically independent Ti atoms are split out into two subgroups with respect to the spin magnetic moment per Ti site: Ti(1)/Ti(3) with a moment of $0.66/-0.67$ μ_B, respectively, and Ti(2)/Ti(4) with $0.04/-0.02$ μ_B. Thus, one of the t_{2g} majority/minority spin states of Ti(1)/Ti(3) becomes occupied (d^1), whereas all other t_{2g} states are pushed by strong Coulomb interaction above the Fermi level. In contrast, all t_{2g} states of Ti(2) and Ti(4) are almost depopulated (d^0) and form bands up to 2.5 eV above the Fermi level. The occupied Ti(1)/Ti(3) states are strongly localized and form a prominent structure with a band width of 0.25 eV just below the Fermi level (see figure 3). The strong Coulomb interaction does not affect the empty Ti e_g states much, which give a predominant contribution between 2.5 and 4.5 eV. The obtained magnetic structure is almost

[8] In fact, the true nonmagnetic ground state caused by the formation of Ti(1)–Ti(3) singets cannot be obtained in the one-electron approach used in the present study. However, the possibility of the formation of the singlet state is strongly supported by the calculated exchange coupling between Ti(1) and Ti(3) cations.

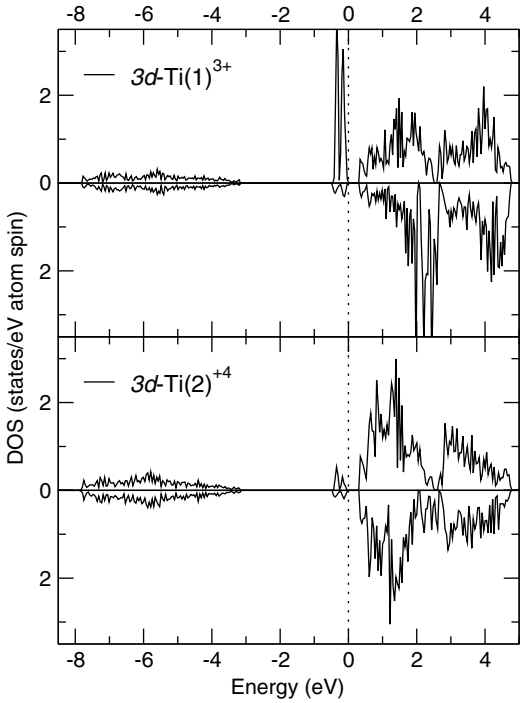

Figure 3. The partial DOS for $Ti(1)^{3+}$ and $Ti(2)^{4+}$ cations are shown. The gap value of 0.29 eV was obtained by LDA + U with $U = 3.0$ eV and $J = 0.8$ eV. The Fermi level is shown by the dotted line. Top and bottom panels correspond to the majority and minority spin states, respectively.

antiferromagnetic, with the spin magnetic moments within $Ti(1)^{3+}$–$Ti(3)^{3+}$ as well as $Ti(2)^{4+}$–$Ti(4)^{4+}$ pairs being of the same magnitude with opposite sign.

An analysis of occupation matrices of $Ti(1)^{3+}/Ti(3)^{3+}$ majority/minority 3d spin states confirms substantial charge disproportionation within the Ti 3d shell. As shown in table 1, one of the t_{2g} states of Ti^{3+} cations (d^1) is occupied with an occupation number of 0.74, whereas the remaining two t_{2g} orbitals have a significantly smaller population of about 0.08. Thus, according to reference [5], we define an orbital order parameter as the largest difference between 3+ and 4+ Ti t_{2g} populations, which amounts to 66% of the ideal ionic charge ordering model. The orbital order parameter clearly shows the existence of substantial charge disproportionation in the Ti 3d shell of Ti_4O_7, which is remarkable because of the complete lack of the total charge separation (see column q in table 1) between 3+ and 4+ Ti cations. The occupation matrices analysis shows that the change in the t_{2g} occupations is very efficiently screened by the rearrangement of the other Ti electrons. A significant portion of the screening charge is provided by Ti e_g states due to the formation of relatively strong σ bonds with O 2p states, which results in an appreciable contribution of the former to the occupied part of the valence band. Ti 4s and 4p states give additional contributions to the screening of the difference in t_{2g} occupations. This leads to complete loss of the disproportionation between the charges at 3+ and 4+ Ti sites.

The occupied t_{2g} Ti^{3+} states are predominantly of d_{xy} character in the local cubic frame (according to that, we later mark the orbital as a d_{xy} orbital). This is illustrated in figure 4, which shows the angular distribution of the majority and minority spin 3d electron density

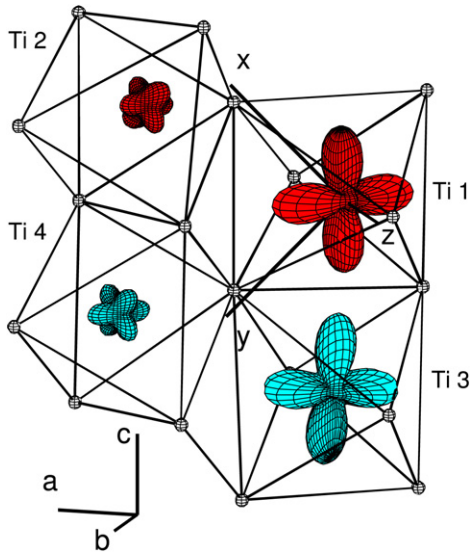

Figure 4. Structure of Ti_4O_7 showing the angular distribution of the majority and minority spin 3d electron density of Ti cations. Red and cyan (light and dark, respectively, on the black and white image) orbitals correspond to the majority and minority 3d spin states, respectively. Oxygen atoms are shown by small spheres. The size of orbital corresponds to its occupancy. X–Y–Z coordinate system corresponds to the local cubic frame.

Table 1. Total (q) and l-projected ($q_{s,p,d}$) charges, magnetic moments (M), and occupation of the most populated t_{2g} orbitals (n) calculated for inequivalent Ti atoms in the low-temperature $P\bar{1}$ phase of Ti_4O_7.

Ti ion	q	q_s	q_p	q_d	M (μ_B)	t_{2g} orbital	n
$Ti(1)^{3+}$	2.27	0.18	0.27	1.83	0.66	$d_{xy\uparrow}$	0.74
$Ti(2)^{4+}$	2.22	0.22	0.33	1.68	0.04		0.08
$Ti(3)^{3+}$	2.16	0.18	0.25	1.74	−0.67	$d_{xy\downarrow}$	0.73
$Ti(4)^{4+}$	2.16	0.21	0.33	1.62	−0.02		0.07

of Ti cations, marked by red and cyan colours (or light and dark on the black and white image), respectively[9]. Since $Ti(1)^{3+}$ and $Ti(3)^{3+}$ cations are antiferromagnetically coupled, the obtained ferro-orbital order is consistent with the formation of a bonding spin-singlet state from the d_{xy} orbitals of two neighbouring Ti(1) and Ti(3) sites. The orientation of occupied Ti^{3+} t_{2g} orbitals is consistent with the largest average Ti–O distance in the plane of t_{2g} orbitals. As shown in table 2, the average Ti(1)–O distance (2.061 Å) in the plane of the d_{xy} orbital is considerably larger than the average distances in the other two yz and zx planes (2.032 and 2.045 Å, respectively). The same is also true for the Ti(3) cation, but in this case the variation in the average Ti(3)–O distances is much smaller (2.047 versus 2.041 and 2.042 Å) and, as a consequence, the out-of-plane rotation of the occupied t_{2g} minority spin orbital is stronger.

Estimation of exchange interaction parameters via the variation of the ground-state energy with respect to the magnetic moment rotation angle [26, 31] results in a strong

[9] The distribution is calculated according to $\rho(\theta,\phi) = \sum_{m,m'} n_{m,m'}\ Y^*_m(\theta,\phi)\ Y_{m'}(\theta,\phi)$, where $n_{m,m'}$ is the occupation matrix of 3d majority states of Ti(1) and 3d minority states of Ti(3) cations. The occupation matrices were calculated using the LDA + U with $U = 3.0$ eV and $J = 0.8$ eV for the low-temperature $P\bar{1}$ phase of Ti_4O_7. $Y_m(\theta,\phi)$ denotes corresponding spherical harmonics.

Table 2. The averaged Ti–O distances in the plane of t_{2g} orbitals ($d_{\text{orb.}}$) and in the oxygen octahedra ($d_{\text{av.}}$) for the $P\bar{1}$ structure of Ti_4O_7. The occupied orbital of the $3d^1$ Ti(1) and Ti(3) 3+ cations is predominantly of d_{xy} character.

Ti atom	orbital	$d_{\text{orb.}}$ (Å)	$d_{\text{av.}}$ (Å)
Ti(1)	d_{xy}	2.061	2.046
	d_{yz}	2.032	
	d_{zx}	2.045	
Ti(2)	d_{xy}	2.012	2.000
	d_{yz}	1.976	
	d_{zx}	2.013	
Ti(3)	d_{xy}	2.047	2.043
	d_{yz}	2.041	
	d_{zx}	2.042	
Ti(4)	d_{xy}	1.973	1.977
	d_{yz}	1.976	
	d_{zx}	1.981	

antiferromagnetic coupling of −1696 K between neighbouring Ti(1) and Ti(3) 3+ cations[10]. The inter-pair $Ti(3)^{3+}$–$Ti(3)^{3+}$ coupling is found to be of −81 K, whereas all other couplings are smaller. This indicates a possible formation of the spin-singlet pairs via direct antiferromagnetic exchange between neighbouring Ti(1) and Ti(3) sites. The contribution of the superexchange via O p orbitals to the Ti(1)–Ti(3) exchange coupling is found to be negligible. This was verified by calculating the exchange coupling constants with the sub-blocks of the LMTO Hamiltonian responsible for the Ti–O hybridization being set to zero. This calculation gives qualitatively the same result for the exchange constants (−1931 K), although the possibility for superexchange via O p orbitals was eliminated.

A strong variation of the exchange coupling constants between different Ti pairs is corraborated by the large difference in corresponding hopping matrix elements evaluated via Fourier transformation from reciprocal space to real space of the Ti t_{2g} LDA Wannier Hamiltonian [32]. Thus, in the low-temerature phase, the amplitude of Ti(1)–Ti(3) intra-pair xy–xy hopping (0.68 eV) is found to be more than three times larger than the rest. The Ti(3)–Ti(3) xy–xy inter-pair hopping (along the a chain) is found to be 0.23 eV, whereas in the b-chain intra/inter-pair hopping integrals are even smaller (0.16 and 0.13 eV, respectively). In contrast, in the high-temperature phase, the amplitudes of hoping integrals between different Ti sites are almost the same (0.23, 0.21, 0.39, and 0.33 eV between 1–3, 2–4, 3–3, and 4–4 Ti sites, respectively).

5. Summary and conclusions

In summary, in the present LDA + U study of the low-temperature $P\bar{1}$ phase of Ti_4O_7 we found a charge-ordered insulating solution with an energy gap of 0.29 eV. The total 3d charge separation is small (less than 0.14), whereas the orbital order parameter defined as the difference between t_{2g} occupancies of Ti^{3+} and Ti^{4+} cations is large and gives direct evidence for charge ordering. Strong covalency of O 2p–Ti 3d σ-type bonds, which results in the partial occupation of Ti e_g states, leads to almost complete loss of the disproportionation between the charges

[10] The exchange coupling parameter J represents the effective pair exchange interaction between Ti atoms with an effective Heisenberg Hamiltonian $H = -\sum_{i>j} J_{ij} S_i \cdot S_j$, where S_i and S_j are spin magnetic moment vectors at sites i and j. Positive (negative) values of J correspond to the ferromagnetic (antiferromagnetic) coupling between sites.

at 3+ and 4+ Ti sites. The occupied t_{2g} states of Ti^{3+} cations are predominantly of d_{xy} character (in the local cubic frame) and form a spin-singlet molecular orbital via strong direct antiferromagnetic exchange coupling between neighbouring Ti(1) and Ti(3) sites of about 1700 K, whereas the role of superexchange is found to be negligible. This is in good agreement with small and temperature-independent magnetic susceptibility in the low-temperature phase of Ti_4O_7.

Acknowledgments

We are grateful to K Schwarz, P Blaha, P Fulde, and D Vollhardt for helpful discussions. The present work was supported in part by Russian Basic Research Foundation Grant (RFFI) nos 04-02-16096, 03-02-39024, the Netherlands Organization for Scientific Research (NWO) 047.016.005, and by the Sonderforschungsbereich 484 of the Deutsche Forschungsgemeinschaft (DFG).

References

[1] Coey M 2004 *Nature* **430** 155
[2] Several reviews of research on the Verwey transition up to 1980 are contained in the special issue of 1980 *Phil. Mag.* B **42**
See also Attfield J P 2006 *Solid State Sci.* **8** 861
[3] Verwey E J W 1939 *Nature* **144** 327
[4] Verwey E J W, Haayman P W and Romeijan F C 1947 *J. Chem. Phys.* **15** 181
[5] Leonov I, Yaresko A N, Antonov V N, Korotin M A and Anisimov V I 2004 *Phys. Rev. Lett.* **93** 146404
Leonov I, Yaresko A N, Antonov V N and Anisimov V I 2006 *Phys. Rev.* B **74** 165117
[6] Horng-Tay Jeng, Guo G Y and Huang D J 2004 *Phys. Rev. Lett.* **93** 156403
[7] Leonov I, Yaresko A N, Antonov V N, Attfield J P and Anisimov V I 2005 *Phys. Rev.* B **72** 014407
[8] Attfield J P, Clarke J F and Perkins D A 1992 *Physica* B **180/181** 581
[9] Attfield J P, Bell A M T, Rodriguez-Martinez L M, Greneche J M, Cernik R J, Clarke J F and Perkins D A 1998 *Nature* **396** 655
[10] Attfield J P, Bell A M T, Rodriguez-Martinez L M, Greneche J M, Retoux R, Leblanc M, Cernik R J, Clarke J F and Perkins D A 1999 *J. Mater. Chem.* **9** 205
[11] Schwingenschlögl U, Eyert V and Eckern U 2003 *Europhys. Lett.* **61** 361
Schwingenschlögl U, Eyert V and Eckern U 2003 *Europhys. Lett.* **64** 682
Schwingenschlögl U and Eyert V 2004 *Ann. Phys., Lpz.* **13** 475
[12] Wentzcovitch R M, Schulz W W and Allen P B 1994 *Phys. Rev. Lett.* **72** 3389
[13] Korotin M A, Skorikov N A and Anisimov V I 2002 *Phys. Met. Metallogr.* **94** 17
[14] Eyert V 2002 *Ann. Phys., Lpz.* **11** 650
[15] Eyert V, Horny R, Höck K-H and Horn S 2000 *J. Phys.: Condens. Matter* **12** 4923
[16] Eyert V 2002 *Europhys. Lett.* **58** 851
[17] Biermann S, Poteryaev A, Lichtenstein A I and Georges A 2005 *Phys. Rev. Lett.* **94** 026404
[18] Bartholomew R F and Frankl D R 1969 *Phys. Rev.* **187** 828
[19] Lakkis S, Schlenker C, Chakraverty B K, Buder R and Marezio M 1976 *Phys. Rev.* B **14** 1429
[20] Marezio M, McWhan D B, Dernier P D and Remeika J P 1972 *Phys. Rev. Lett.* **28** 1390
[21] Marezio M and Dernier P D 1971 *J. Solid State Chem.* **3** 340
[22] Hodeau J L and Marezio M 1979 *J. Solid State Chem.* **29** 47
[23] LePage Y and Marezio M 1984 *J. Solid State Chem.* **53** 13
[24] Eyert V, Schwingenschlögl U and Eckern U 2004 *Chem. Phys. Lett.* **390** 151
[25] Andersen O K 1975 *Phys. Rev.* B **12** 3060
[26] Liechtenstein A I, Anisimov V I and Zaanen J 1995 *Phys. Rev.* B **52** R5467
[27] Marezio M, McWhan D B, Dernier P D and Remeika J P 1973 *J. Solid State Chem.* **6** 213
[28] Streltsov S V, Mylnikova A S, Shorikov A O, Pchelkina Z V, Khomskii D I and Anisimov V I 2005 *Phys. Rev.* B **71** 245114
Solovyev I, Hamada N and Terakura K 1996 *Phys. Rev.* B **53** 7158
[29] Kaplan D, Schlenker C and Since J J 1997 *Phil. Mag.* **36** 1275

Abbate M, Potze R, Sawatzky G A, Schlenker C, Lin H J, Tjeng L H, Chen C T, Teehan D and Turner T S 1995 *Phys. Rev.* B **51** 10150
Abbate M, Potze R, Sawatzky G A, Schlenker C, Teehan D and Turner T S 1995 *Solid State Commun.* **94** 465
[30] García J, Subías G, Proietti M G, Renevier H, Joly Y, Hodeau J L, Blasco J, Sánchez M C and Bérar J F 2000 *Phys. Rev. Lett.* **85** 578
[31] Anisimov V I, Aryasetiawan F and Lichtenstein A 1997 *J. Phys.: Condens. Matter* **9** 767
[32] Anisimov V I, Kondakov D E, Kozhevnikov A V, Nekrasov I A, Pchelkina Z V, Allen J W, Mo S-K, Kim H-D, Metcalf P, Suga S, Sekiyama S, Keller G, Leonov I, Ren X and Vollhardt D 2005 *Phys. Rev.* B **71** 125119